An *ab initio* study of $WO_3$ under pressure up to 30 GPa



2003 J. Phys.: Condens. Matter 15 3121

(http://iopscience.iop.org/0953-8984/15/19/313)

INSTITUTE OF PHYSICS PUBLISHING JOURNAL OF PHYSICS: CONDENSED MATTER

J. Phys.: Condens. Matter **15** (2003) 3121–3133 PII: S0953-8984(03)59378-X

# An *ab initio* study of $WO_3$ under pressure up to 30 GPa

**T Pagnier**[1] **and A Pasturel**[2]

[1] LEPMI-ENSEEG, 1130 rue de la Piscine BP 75, F-38402 Saint Martin d'Hères, France
[2] LPMMC, Maison des Magistères, BP 166 CNRS, 38042 Grenoble Cedex 09, France

Received 10 February 2003
Published 6 May 2003
Online at stacks.iop.org/JPhysCM/15/3121

**Abstract**

High-pressure polymorphs of $WO_3$ have been studied with a first-principles pseudopotential method. The medium-range (0.01–20 GPa) and high-range (20–30 GPa) polymorphs have been characterized and are compared with recent experimental results. The main new feature is the appearance of a sevenfold coordinated tungsten in the high-pressure polymorph. The subtle phase transitions that were induced from Raman spectra evolutions have not been confirmed. However, changes in the W–O distances and O–W–O and W–O–W angles may explain the changes in Raman spectra.

## 1. Introduction

Tungsten trioxide $WO_3$ has attracted much interest because of its potential for technological applications. It first received attention because of its electrochromic properties [1]. In the past few years, its gas sensing abilities have also been extensively studied [2, 3].

The structure of $WO_3$ can be viewed on the basis of a $ABO_3$ perovskite in which the A ions, located between the $WO_6$ octahedra, have been removed. This compound displays an important polymorphism as a function of pressure and temperature, depending upon distortion and tilting of the corner-sharing octahedra.

At atmospheric pressure and room temperature, it is established that the stable phase is monoclinic ($P2_1/n$) with eight formula units per unit cell. From room temperature to 1000 °C, four other phases have been found [4], an orthorhombic phase ($Pbcn$) between 350 and 720 °C, a monoclinic one ($P2_1/c$) between 720 and 800 °C, a tetragonal one ($P4/ncc$) between 800 and 900 °C and another tetragonal phase ($P4/nmm$) above 900 °C.

At high pressures, a variety of phase transitions have been observed but there is yet no general agreement about the high-pressure phase diagram. At low pressure, i.e. 0.15 GPa, Salje and Hoppmann [5] observed a complete transition into another monoclinic phase with space group $Pc$. However, in another study, Xu *et al* [6] conclude on the occurrence of a $P2_1/c$ phase above 0.57 GPa, distinct from the monoclinic phase reported previously. Finally, from Raman investigations, Souza Filho *et al* [7] conclude on a complete transformation above 1.4 GPa but without any arguments to clarify the group symmetry of this high-pressure phase. A theoretical study [8] based on *ab initio* calculations concludes on the $P2_1/c$ structure as the thermodynamic

  

stable structure. Very recently, two studies, one based on Raman spectroscopy [9] and the other one on x-ray diffraction (XRD) [10], have investigated the high-pressure behaviour of $WO_3$ up to 30 and 40 GPa respectively. Both studies confirm the phase transition taking place at about 0.1 GPa. Moreover, another phase transition is evidenced at about 22 GPa in Raman investigations and at about 24 GPa in XRD experiments. However the two spectral anomalies observed around 3 and 10 GPa in the Raman spectra are not confirmed by the XRD study.

We therefore intended to extend the previous theoretical study of $WO_3$ by de Wijs *et al* [8] to higher pressures, in order to understand the different trends observed by these recent Raman spectroscopy and XRD studies. This study must allow us to confirm or not the existence of phase transitions at 3 and 10 GPa. Section 2 presents details of the calculation method. In section 3 results of the calculations on various structures are presented. More particularly, this study reports results for the room-temperature atmospheric-pressure phase (denoted RP hereafter) and the two high-pressure structures (HP1 and HP2). Conclusions are found in section 4.

## 2. Calculation method

All calculations were performed using the *ab initio* program VASP [11] and we follow the prescriptions given by de Wijs *et al* [8]. Ultrasoft pseudopotentials provided with the program were used, with a frozen $[Xe]4f^{14}$ and $1s^2$ core for W and O, respectively. Nonlinear core corrections were applied to W. Exchange and correlation were treated with the local-density functional of Ceperley and Alder [12] since structural characteristics of $WO_3$ polymorphs seem to be better described by the LDA [8].

For each structure, the equilibrium volume is obtained from a Birch–Murnaghan fit to a set of calculations at various fixed volumes. For each volume, the cell parameters and atomic positions were allowed to relax according to the phase symmetry using conjugate-gradient minimizations as implemented in the VASP program optimization routines. During this step, the energy cut-off was held at 396 eV. The $k$-point meshes for the different phases have been chosen following de Wijs' arguments [8]. Such $k$-point meshes give an accuracy for total energies better than 1 meV/atom.

In order to compare XRD experimental results with our calculations, we have used the volume parameter in both cases. For comparisons with Raman experiments, we have used the $P$–$V$ relation found experimentally by XRD (see figure 1) to translate pressure into volume.

## 3. Results

### *3.1. RP phase*

For the $P21/n$ monoclinic RP phase with eight formula units per unit cell, the crystal energy versus volume is shown in figure 2. The minimum energy $E_0$, volume at minimum $V_0$ and bulk modulus $K$ were obtained by fitting the data to the Birch–Murnaghan equation:

$$E = E_0 + \frac{9}{8} K V_0 \left[ \left( \frac{V_0}{V} \right)^{2/3} - 1 \right]^2. \tag{1}$$

Table 1 gives the values of $E_0$, $V_0$ and $K$. The low value of $K$ (40 GPa) is comparable to that obtained in [8] and confirms the softness of this material. The cell parameters are shown as a function of volume in figure 3. For volumes higher than the equilibrium volume, the monoclinic distortion vanishes, as shown by the $\beta$ angle shifting to 90°. The cell becomes

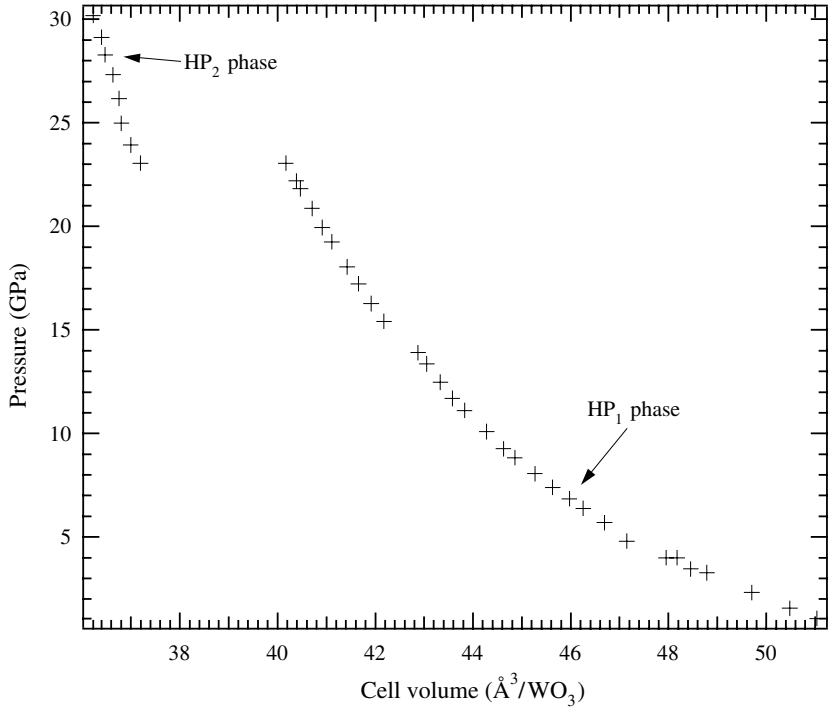


**Figure 1.** Experimental relationship between pressure and cell volume (expressed in $Å^3/WO_3$) from [10].

**Table 1.** Equilibrium energy $E_0$, volume $V_0$ and bulk modulus $K$ for the three phases investigated and comparisons with previous works.

| | $E_0$ (eV/$WO_3$) | $V_0$ ($Å^3/WO_3$) | $K$ (GPa) |
|---|---|---|---|
| | | Monoclinic RP phase | |
| Exp.[a] | | 52.96 | |
| This work | −39.740 | 51.64 | 39.18 |
| | | Monoclinic HP1 phase | |
| Exp. 1[b] | | | 44.5 ($K' = 2.5$) |
| Exp. 2[c] | | 52.725 | 27 ($K' = 9.4$) |
| [d] | | 51.95 | 45 ($K' = 2.5$) |
| This work | −39.736 | 51.40 | 40.68 |
| | | Monoclinic HP2 phase | |
| Exp.[c] | | 37.025 | 296 |
| This work | −39.170 | 40.78 | 150.76 |

[a] Reference [17].
[b] Reference [6].
[c] Reference [10].
[d] Pressure range limited to 1.06–6 GPa.

roughly tetragonal, with three relatively close axes (for a volume of 56 $Å^3/WO_3$, $a = 7.51$ Å, $b = 7.66$ Å and $c = 7.79$ Å). For volumes lower than that corresponding to the atmospheric pressure, the cell parameters follow a quasi-linear variation, except for the last calculated point

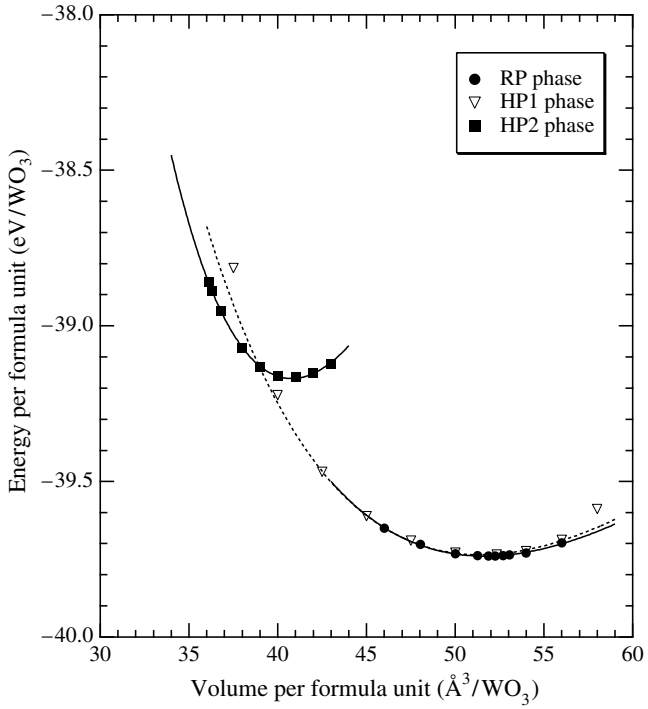


**Figure 2.** Crystal energies as a function of volume for the three phases under investigation.

at 46 $Å^3/WO_3$ for which $a$ and $b$ parameters come closer. However this volume is far below that of the RP–HP1 transition.

Figure 4 shows schematically the atomic positions in the RP phase and gives the atom labelling used in the text. Along the $a$ axis, we find the sequence W1–O1–W2–O2 with short W1–O2 and W2–O1 distances. Along the $b$ axis, we find W1–O3–W1–O3 and W2–O4–W2–O4 sequences, with alternating short and long W–O bonds. Along the $c$ axis, sequences are in the form W1–O6–W2–O5 and W2–O6–W1–O5, with short W1–O6 and W2–O5 bonds. Table 2 gives the atomic positions in the asymmetric unit [13] for a volume of 51.87 $Å^3/WO_3$. Figure 5 shows W–O bond lengths and selected O–W–O angles, which together describe the shape and distortion of the $WO_6$ octahedra. The first comment is that W1 and W2 atoms, and their octahedral environments, are very similar. This suggests that another structure with a higher symmetry would have about the same energy (see below). In the whole range, except for the lowest volume ($V = 46\ Å^3/WO_3$), changes in the octahedra are very minor. The splittings into long and short bonds are of different magnitudes along the $a$, $b$, and $c$ directions and only small modifications are seen as a function of the volume; under expansion, only a few W–O bonds are elongated (along the $c$ axis and two in the $a$, $b$ plane); under compression almost all nearest-neighbour distances remain constant. Indeed, the O–W–O angles are also hardly affected by the volume change.

In contrast, the octahedron tilt is strongly dependent upon volume, and therefore on pressure (figure 6). This is demonstrated by the strong volume dependence of the W–O–W angles, that determine the relative orientation of octahedra as already mentioned in [8]. Most of the volume change upon pressure is therefore due to a compaction of (relatively) stable octahedra.

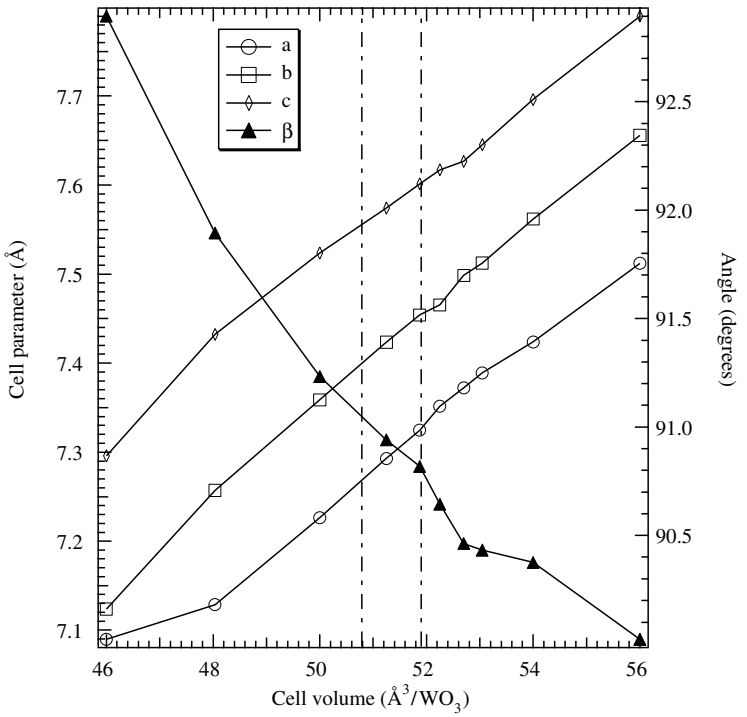


**Figure 3.** Cell parameters as a function of cell volume in the RP phase. Vertical dotted lines indicate the domain of existence of this phase.

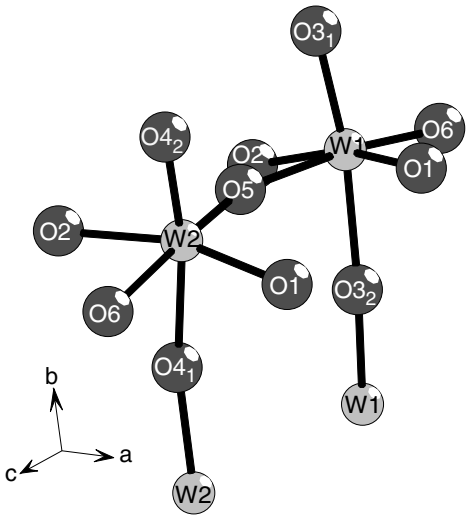


**Figure 4.** Schematic view of the room-pressure (RP) phase. Ion labels are those used throughout the manuscript.

### *3.2. HP1 phase*

The HP1 phase is monoclinic, space group $P21/c$, with four formula units per unit cell. The energy versus volume curve (see figure 2) is very close to that of the RP phase. Indeed,

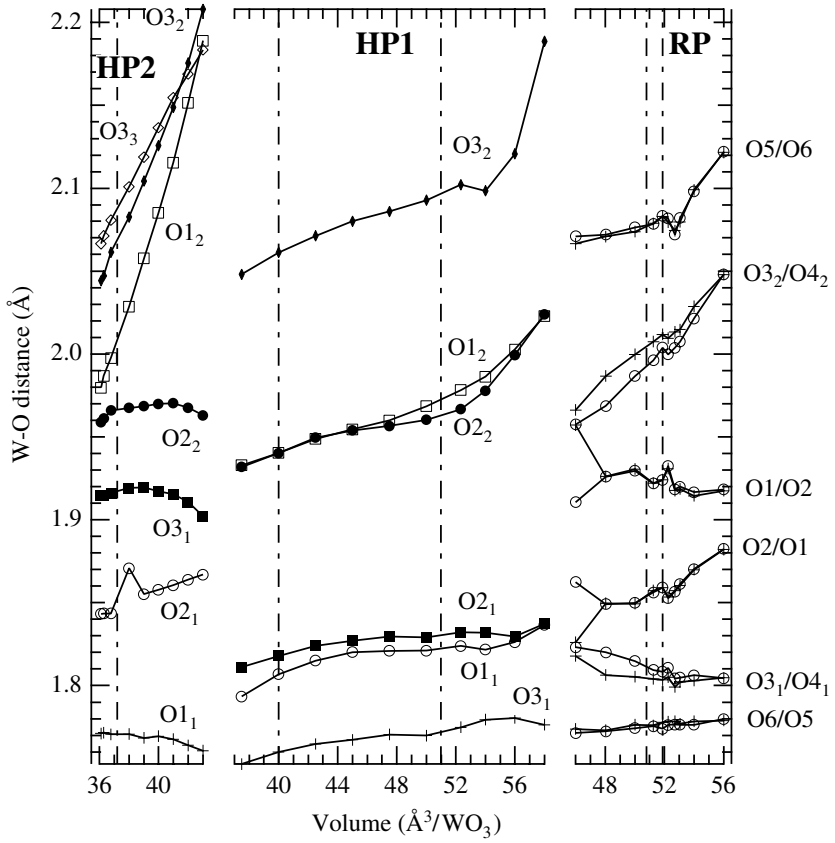


**Figure 5.** W–O bond lengths in the three phases as a function of cell volume. Atom labels are those of figures 4, 9 and 11. Vertical dotted lines indicate the domain of existence of each phase (50.8–51.9 Å$^3$/WO$_3$ for the RP phase, 40–51 for the HP1 phase and 36–37.2 for the HP2 phase). For the RP phase, W1–O bonds are indicated by + symbols and the oxygen atom involved is the first one written. W2–O bonds are indicated by circles and the oxygen atom is the second one.

calculated values for $V_0$, $E_0$ and $K$ (table 1) are very similar to those of the RP phase. The calculated $K$ bulk modulus is close to the experimental values of Xu *et al* [6] and of Bouvier *et al* [10] when a limited range is used (table 1). Let us mention that at high and low volumes there is a significant deviation from the Birch–Murnaghan equation, which may explain the $K$-determination dependence on the volume range [10].

The calculated cell parameters are shown in figure 8 and display a very good agreement with experimental XRD data [10] in the whole volume range. Figure 9 shows a schematic view of the HP1 phase. W–O bond lengths and selected O–W–O angles are shown in figures 5 and 6 respectively.

As for the RP phase, the internal parameters of the octahedron do not change significantly between 40 and 51 Å$^3$/WO$_3$. A long–short splitting occurs for all three directions and it is more pronounced along the $c$-axis. Under compression, all nearest-neighbour distances remain almost constant and the O–W–O angles also display a weak variation as a function of volume. However, there are some subtle features which appear near 45 Å$^3$/WO$_3$. In this region, a change in the slope is observed for most parameters, especially for the W–O1$_1$ distance and the angles O1$_1$–W–O2$_1$ (its slope becomes negative), O1$_1$–W–O2$_2$ and O2$_1$–W–O1$_2$. Moreover, the

**Table 2.** Atomic positions in the asymmetric unit [13] for the three studied phases.

| | RP phase | HP1 phase | HP2 phase |
|---|---|---|---|
| Cell volume ($Å^3/WO_3$) | 51.871 | 50 | 36.7875 |
| W1 | 0.25497 | 0.25517 | 0.76677 |
| | 0.02129 | 0.26554 | 0.34237 |
| | 0.28134 | 0.28534 | 0.93812 |
| W2 | 0.24481 | | |
| | 0.02531 | | |
| | 0.77915 | | |
| O1 | 0.00085 | 0.96306 | 0.54662 |
| | 0.03687 | 0.04399 | 0.63127 |
| | 0.21537 | 0.20802 | 0.71878 |
| O2 | 0.99827 | 0.44792 | 0.75834 |
| | 0.46291 | 0.95886 | 0.03580 |
| | 0.21705 | 0.20909 | 0.73785 |
| O3 | 0.28432 | 0.25242 | 0.09906 |
| | 0.26152 | 0.33335 | 0.51379 |
| | 0.28025 | 0.01084 | 0.24837 |
| O4 | 0.20882 | | |
| | 0.26064 | | |
| | 0.73237 | | |
| O5 | 0.28495 | | |
| | 0.03606 | | |
| | 0.00962 | | |
| O6 | 0.28459 | | |
| | 0.48586 | | |
| | 0.99109 | | |

two distances W–$O1_2$ and W–$O2_2$ become similar in this region. It is interesting to notice that Boulova *et al* [9] observed changes in the slope of some Raman bands with pressure near 10 GPa, which corresponds to 44 $Å^3/WO_3$ (figure 1 of [9]). It is also interesting to emphasize that the $O1_1$–W–$O2_2$ and $O2_1$–W–$O1_2$ angles, which are almost equal at large volume, become different between 50 and 48 $Å^3/WO_3$. All these features may explain the changes in the Raman spectra observed in [9] and confirm the XRD evidence of a single phase in this pressure domain [10].

As for the RP phase, the crystallographic consequences of the volume variation can be seen in the relative orientation of neighbouring octahedra (figure 7). As for the RP phase, the values of W–O–W angles are strongly volume dependent. They also show variations which may explain the Raman spectrum changes in the low-energy part of the spectra. The most striking change is the W–O3–W angle: it is close to the W–O1–W angle between 45 and 50 $Å^3/WO_3$ and becomes equal to the W–O2–W angle at a volume of 41 $Å^3/WO_3$.

### *3.3. HP2 phase*

As discussed in the introduction, a new phase, called HP2, appears experimentally at pressures higher than about 21 GPa [9, 10]. Raman spectra [9] indicate a strong change between HP1 and HP2 phases. By XRD [10], only the space group and the cell parameters were determined. Atomic positions for W atoms were also provided. Starting with these data, a numerical relaxation shows that W atom positions are shifted from their initial $(x, y, z)$ positions to the

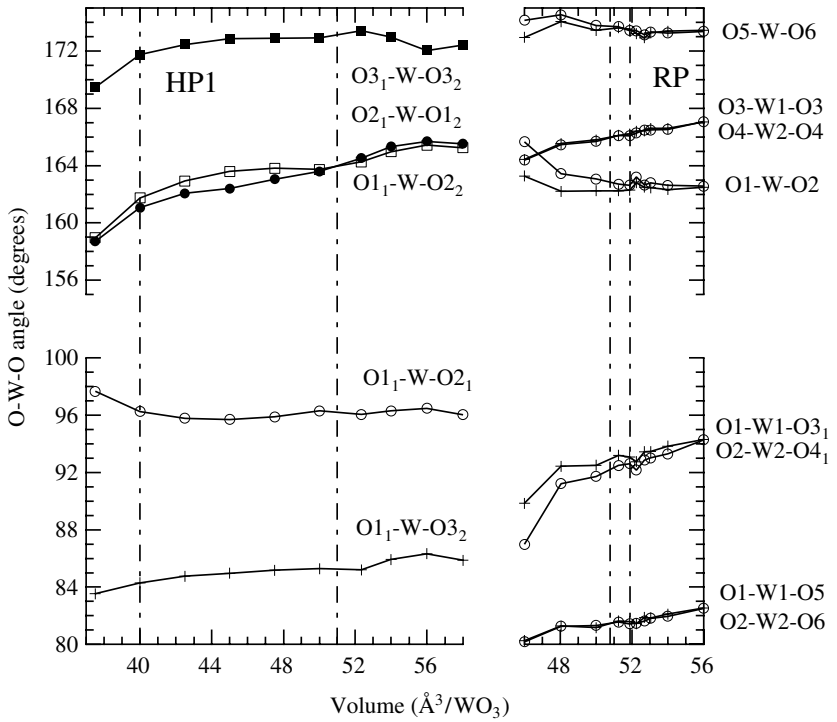


**Figure 6.** Internal coordinates describing octahedral deformations in the RP and HP1 phases. Atom labels are those of figures 4 and 9. Vertical dotted lines indicate the domain of existence of each phase.

**Table 3.** Data calculated from XRD pattern [10] and *ab initio* results for the HP2 phase. Cell parameters $a, b$ and $c$ are in ångströms, $\beta$ is in degrees. The W position (general position) is in fractional coordinates. Data from [10], which were published in the $P2_1/a$ description of the $P2_1/c$ space group, were translated into $P2_1/c$ for comparison with *ab initio* results.

| | XRD | VASP |
|---|---|---|
| $a$ | 7.2971 | 7.255 4 |
| $b$ | 4.5770 | 4.596 36 |
| $c$ | 6.1731 | 6.144 0 |
| $\beta$ | 134.46 | 134.09 |
| $Wx$ | 0.768 13 | 0.766 77 |
| $Wy$ | 0.160 54 | 0.342 37 |
| $Wz$ | 0.929 19 | 0.938 12 |

new $(x, 1/2 - y, z)$ positions (table 3). A comparison of the XRD pattern with the *ab initio* values for cell parameters and atomic positions reveals that these last values were at least as correct as the previous ones to interpret the XRD pattern [14].

The energy versus volume data are shown in figure 2. A Birch–Murnaghan fit gives the value of 150 GPa for $K$ and so the HP2 phase appears much harder than the RP and HP1 phases. Moreover, the volume change at the transition is important. The common tangent rule [15] gives a transition volume of 40.97 Å$^3$/WO$_3$ in the HP1 phase and 37.57 Å$^3$/WO$_3$ in the HP2 phase, giving a volume change of 8.30%. These data are very similar to those obtained by Bouvier *et al* [10], who found 40.17 Å$^3$/WO$_3$, 37.20 Å$^3$/WO$_3$ and 7.4%, respectively.

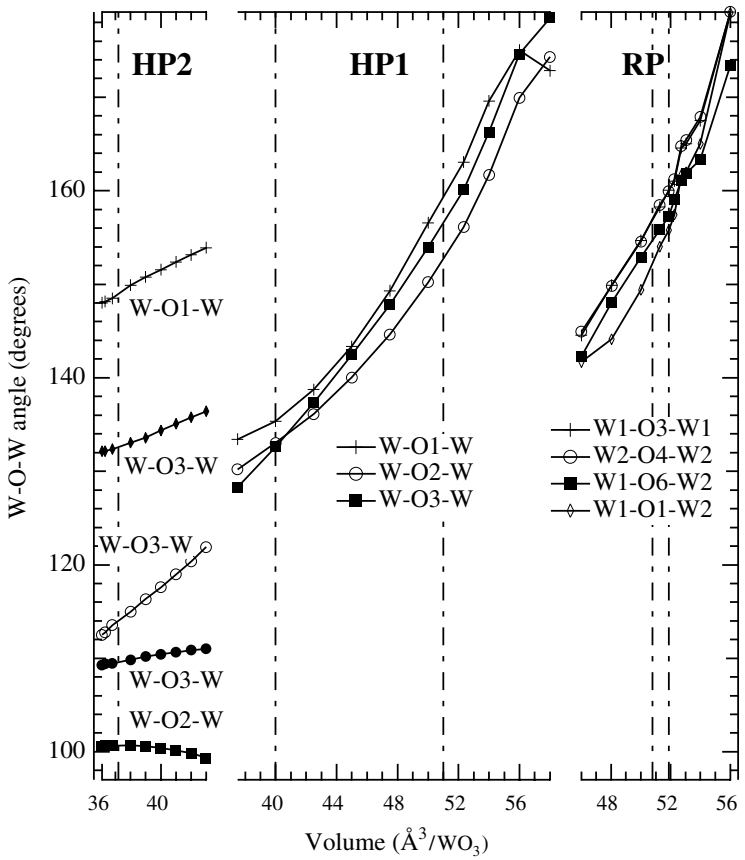


**Figure 7.** Internal coordinates describing octahedral tilting in the three phases. Atom labels are those of figures 4, 9 and 11. Vertical dotted lines indicate the domain of existence of each phase.

Figure 10 shows the changes in cell parameters as a function of the cell volume. Experimental data are well reproduced, including the maximum in the $\beta$ angle observed near 36.5 Å$^3$/$WO_3$. Below 36 Å$^3$/$WO_3$, a phase transition is experimentally observed, leading to a new monoclinic structure with a cell doubling [10]. Our calculations indicate that the calculated cell parameters show an abrupt change at this volume, indicating that the HP2 structure becomes unstable, even without cell doubling. This transition and the structure of the HP3 phase will be the subject of a forthcoming paper [16].

The HP2 phase structure appears to be very different to that of the HP1 phase. Each tungsten atom has now seven tungsten nearest neighbours, three located at about 3.20 Å and the four remaining W at about 3.64 Å. This sevenfold coordination is also observed for oxygen atoms surrounding W: two O1, two O2 and three O3 atoms are located at distances lower than 2.10 Å from W. O1 and O2 atoms have two tungsten nearest neighbours, while O3 atoms have three of them. Figure 11 shows a schematic view of the structure. Polyhedra either share an O1 or an O3 atom or share an O2–O3 or an O3–O3 edge.

Changes in the W–O bond lengths are shown in figure 5. Two different behaviours can be seen: the four shortest bonds remain almost constant as for the RP and HP1 phases. In contrast, the three longest bonds shorten strongly as the volume decreases. It is an indication that the variations of volume now have an influence on the oxygen polyhedron around the

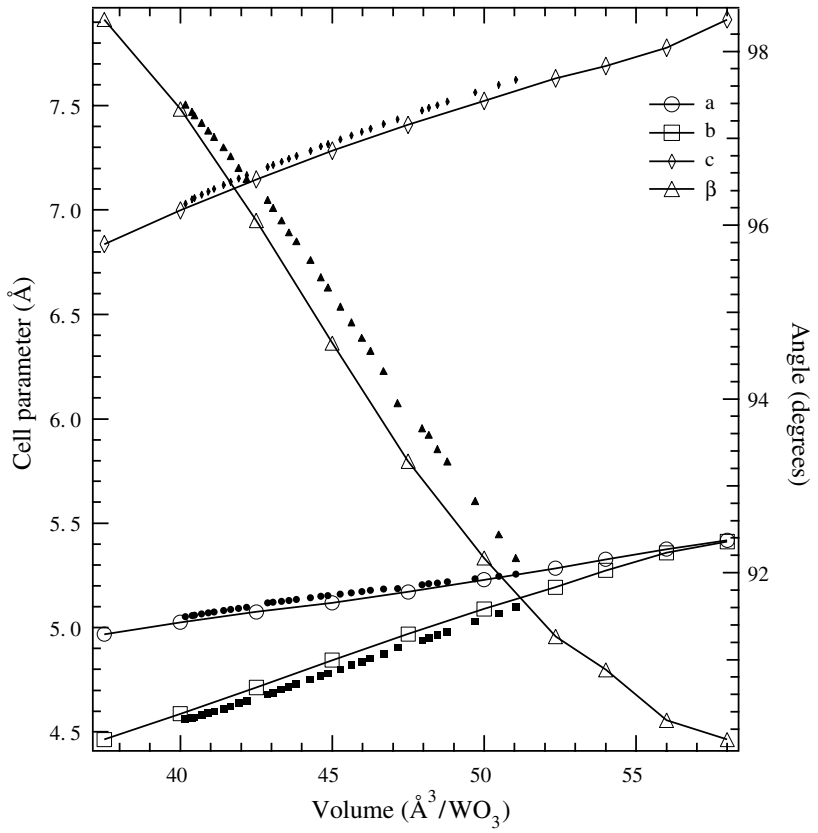


**Figure 8.** Cell parameters as a function of volume in the HP1 phase. Full symbols: experimental data from [10]. Open symbols: calculated values.

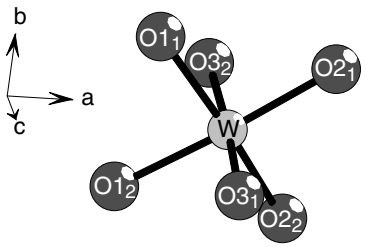


**Figure 9.** Schematic view of the HP1 phase. Ion labels are those used throughout the manuscript.

W atoms. The O–W–O internal bond angles are not really affected either by the changes of volume: three of them change by more than 6° in the whole range, and for most of the other bonds the change is less than 3°. Simultaneously, the W–O–W angles (figure 7) show a limited change, as compared to the changes observed in the RP and HP1 phases. This new behaviour may be explained by the fact that the oxygen polyhedra around W atoms share edges now; consequently, it is more difficult to change their relative orientation.

Then the change in volume is not only due to the angle tilting as in the RP and HP1 phases, but also to the reduction of strong, partially covalent bond distances. This explains

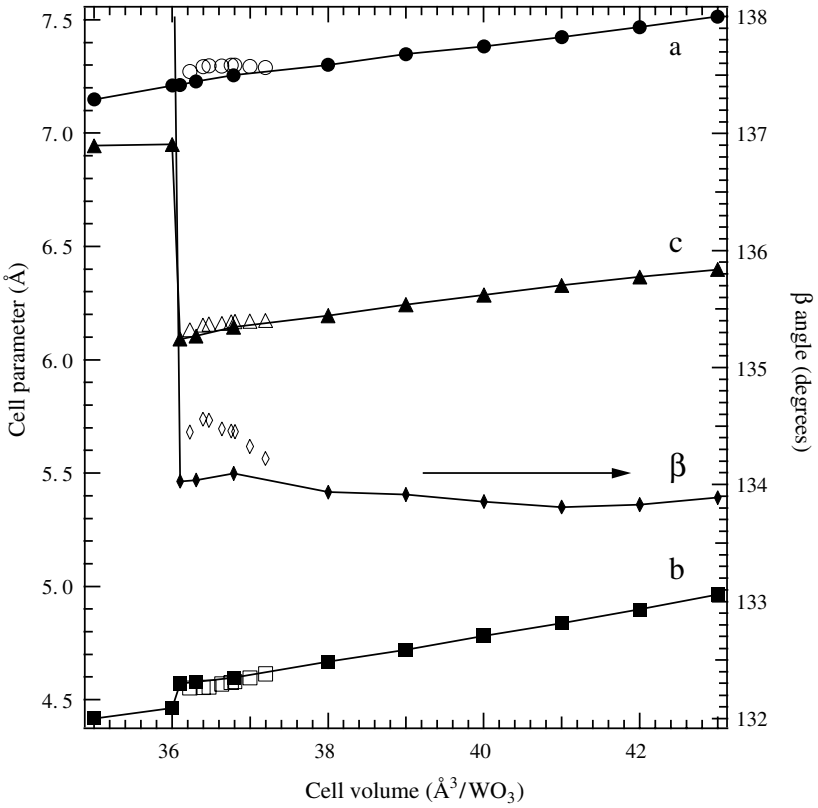


**Figure 10.** Cell parameters as a function of cell volume in the HP2 phase. Open symbols: experimental data from [10]. Filled symbols: calculated values.

the strong increase in the bulk modulus observed in the HP2 phase. Nevertheless, the bulk modulus of a hypothetical cubic phase, computed by *ab initio* methods [8], is still much higher (around 320 GPa). In this particular case, compression results solely in a reduction of the W–O distance. In the case of the HP2 phase, the bulk modulus corresponds to a mixture of shortening W–O bonds and polyhedral tilting.

## 4. Conclusion

*Ab initio* calculations of the structure of $WO_3$ under pressure have confirmed the existence of two polymorphs between 0 and 30 GPa as seen in XRD measurements [10], and the sequence of phase transitions with increasing pressure is

$$P21/n,\ Z = 8 \rightarrow P21/c,\ Z = 4 \rightarrow P21/c,\ Z = 4.$$

The structural determinations of the RP and HP1 phases are in complete agreement with the theoretical results published by de Wijs *et al* [8] and the most recent experimental data [9, 10]. The full determination of the HP2 phase has been obtained. The main result is the low compressibility of this high-pressure phase, which can be related to the compression of the oxygen octahedra themselves through WO bonds. Such a compression leads to a sevenfold coordination for W atoms.

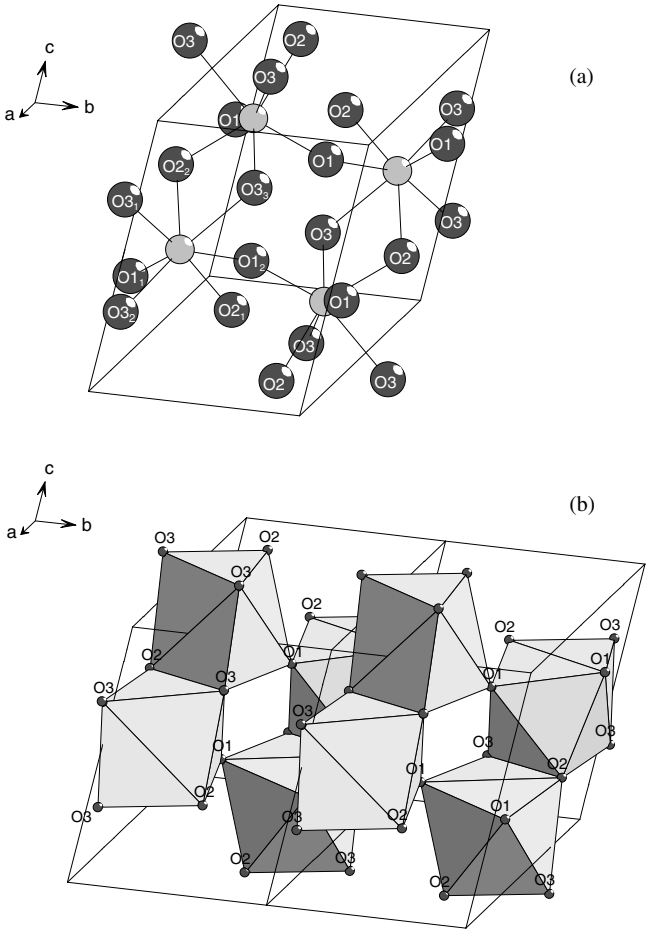


**Figure 11.** Schematic view of the HP2 phase. (a) Description in terms of W–O bonds. Oxygen atom labels are those used throughout the manuscript. (b) View of polyhedra showing edge-sharing polyhedra through O2–O3 and O3–O3 edges and corner-sharing polyhedra through O1 corners.

## Acknowledgments

We thank very much G Lucazeau for helpful discussions and P Bouvier for providing the x-ray diffraction results and for his assistance in the structure drawings.

## References

[1] Grandqvist C G 2000 *Sol. Energy Mater. Sol. Cells* **60** 201
[2] Solis J L, Saukko S, Kish L B, Granqvist C G and Lantto V 2001 *Sensors Actuators* B **77** 316–21
[3] Marquis B T and Vetelino J F 2001 *Sensors Actuators* B **77** 100–10
[4] Howard C J, Luca V and Knight K S 2002 *J. Phys.: Condens. Matter* **14** 377
[5] Salje E and Hoppmann G 1980 *High Temp. High Pressure* **12** 213–16
[6] Xu Y, Carlson S and Norrestam R 1997 *J. Solid State Chem.* **132** 123–30
[7] Souza Filho A G *et al* 2000 *Phys. Rev.* B **62** 3699–703
[8] de Wijs G A, de Boer K, de Groot R A and Kresse G 1999 *Phys. Rev.* B **59** 2684–93
[9] Boulova M, Rosman N, Bouvier P and Lucazeau G 2002 *J. Phys.: Condens. Matter* **14** 5849–63

[10] Bouvier P, Crichton W, Boulova M and Lucazeau G 2002 *J. Phys.: Condens. Matter* **14** 6605–17
[11] Kresse G and Furthmüller J 1996 *Phys. Rev.* B **54** 11169–86
[12] Ceperley D M and Alder B J 1980 *Phys. Rev. Lett.* **45** 566
[13] Hahn T (ed) 1989 *International Tables for Crystallography vol A Space-Group Symmetry* (Dordrecht: Kluwer)
[14] Bouvier P 2002 private communication
[15] Hafner J 1987 *From Hamiltonians to Phase Diagrams* (Berlin: Springer)
[16] Pagnier T *et al* 2003 at press
[17] Loopstra B O and Rietveld H M 1969 *Acta Crystallogr.* B **25** 1420–1